Available online at www.sciencedirect.com
ScienceDirect
Journal of Photochemistry and Photobiology A: Chemistry 192 (2007) 152–158
Journal of Photochemistry and Photobiology A:Chemistry
www.elsevier.com/locate/jphotochem

Probing the interaction of ellagic acid with human serum albumin: A fluorescence spectroscopic study

Ranjan Kumar Nanda [a], Nilmoni Sarkar [b], Rintu Banerjee [a,*]

[a] *Microbial Biotechnology and Downstream Processing Laboratory, Agricultural and Food Engineering Department, Indian Institute of Technology, Kharagpur 721302, India*
[b] *Department of Chemistry, Indian Institute of Technology, Kharagpur 721302, India*

Received 9 February 2007; received in revised form 8 May 2007; accepted 16 May 2007
Available online 18 May 2007

Abstract

Human serum albumin (HSA) is a principal plasma protein, carries the drug molecules to target sites in human body. Ellagic acid (EA) derived from ellagitannins plays an important role as a drug because of its unique pharmacological properties. The interactions between EA and HSA were studied by fluorescence spectroscopic techniques under similar to human physiologic conditions. The binding parameters have been evaluated by fluorescence quenching methods. The results proved the mechanism of fluorescence quenching of HSA while interacting with EA is due to the formation of EA–HSA complex formation. The thermodynamic parameters like ΔH and ΔS were calculated to be −17.32 kJ/mol and 34.91 J/mol/K, respectively, which proves the involvement of weak interactive forces like hydrogen and hydrophobic bonds during the interaction. Molecular docking study shows hydrogen-bonding distance between EA and HSA molecule. The distance r between donor (HSA) and acceptor (EA) was obtained according to the Forster's theory of non-radiative energy transfer and found to be 1.96 nm. This study will give an insight on the evaluation of the drug stability during transport and releasing efficiency at the target site in human physiological conditions.

Keywords: Ellagic acid; Human serum albumin; Fluorescence quenching; Förster resonance energy transfer

1. Introduction

Human serum albumin (HSA) is present in blood plasma abundantly (60%) and structurally well characterized [1–3]. The principal function of HSA is to transport fatty acids as well as broad range of drug molecules to its molecular targets [4,5]. The crystallographic analysis revealed that HSA is composed of 585 amino acid residues with three similar α-helical domains (I, II and III), each containing two sub-domains (A and B), stabilized by 17 disulphide bridges and presence of a single tryptophan residue (Trp214) [6–10]. Two hydrophobic pockets are present in sub-domains IIA and IIIA, which accommodate the aromatic and heterocyclic ligands (drugs and bioactive molecules) to bind reversibly [11–13]. Albumins increase the apparent solubility of hydrophobic drugs in plasma. This property makes HSA an important and dominant regulator in pharmacokinetic behavior of many drugs [14].

Ellagic acid (EA; molecular structure; Fig. 1) is a polyphenol found at high concentrations in a number of fruits like grapes, strawberries, blacks currants and raspberries and shows a variety of biological activities including antioxidant, anti-inflammatory and anti-fibrosis. Recently dietary polyphenols are receiving increasing attention as potential protectors against a variety of human diseases like hepatitis B virus (HBV) and cancer in animal models [15,16]. EA blocks hepatitis 'e' antigen (HBeAg) secretion in a HBV infected cell line and HBeAg transgenic mice. This work suggested the therapeutic use of EA as HBV carriers, since it overrules the viral strategy to guarantee HBV infection [17]. Anti-apoptotic activity of EA in normal human peripheral blood mononuclear cells is studied and has a Bcl-2 independent mechanism hypothesized by [18].

Reports are available, identifying EA to a naturally occurring tannic acid derivative, as a novel potent CK2 inhibitor using a virtual screening approach. EA is found to be the most potent

* Corresponding author. Tel.: +91 3222283104; fax: +91 3222255303.
E-mail address: rb@iitkgp.ac.in (R. Banerjee).

1010-6030/$ – see front matter © 2007 Elsevier B.V. All rights reserved.
doi:10.1016/j.jphotochem.2007.05.018

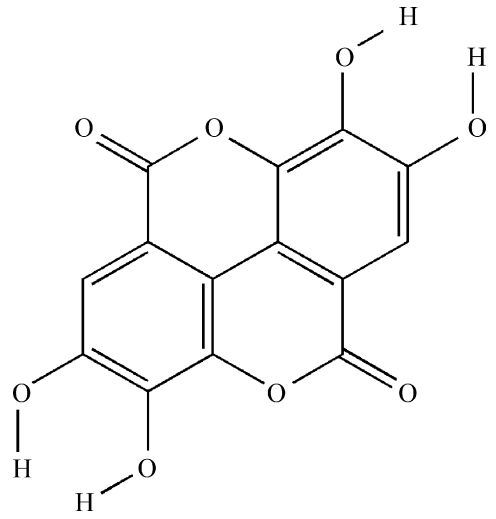

Fig. 1. Molecular structure of ellagic acid.

known CK2 inhibitor with an inhibitor constant (K_i) of 20 nM [19]. Inhibition of mutagenesis through DNA masking and carcinogenesis by arresting G1 phase of cancer cell, was observed in presence of EA [20]. EA acts as a potent antioxidant and reduces heart diseases, birth defects, liver fibrosis and facilitates wound healing. EA is evaluated to be a potent antiestrogen in MCF-7 breast cancer-derived cells by increasing, like the pure estrogen antagonist ICI 182780, insulin-like growth factor binding protein 3 (IGFBP-3) levels [21].

The study of the molecular interactions taking place between ligand and macromolecule, during drug transport and the type of interaction involved, commands the releasing efficiency from the carrier molecule is necessary to predict the effectiveness of a drug molecule. EA quenches the intrinsic fluorescence of bovine serum albumin (BSA) and results a change in conformation with a strong binding constant and weaker tryptophan quenching than tannic acid has been reported [22]. However, detailed investigations of the interaction of HSA with EA have not been yet conducted. Because of wide application of EA in health sciences, information on the interaction study with HSA will give deep insight of its pharmacological applications. In the present report, fluorescence spectroscopy, a nondestructive and powerful method is used to study and understand the interaction involves between the macromolecule and ligand under physiological conditions.

2. Materials and methods

2.1. Materials

HSA and EA were procured from Sigma Aldrich Chemical Pvt. Ltd. (USA). Chemicals like sodium dihydrogen phosphate, disodium hydrogen phosphate, sodium chloride and other involved in the experiments were all of analytical grade. Solutions were prepared using milli Q water. Sodium phosphate buffer saline (0.1 mol L^{-1}, 0.15 mol L^{-1} NaCl, pH 7.4 ± 0.1) was used. EA and HSA solutions (5 μM) were prepared in the sodium phosphate buffer saline. All stock solutions were stored at 0–4 °C.

2.2. Equipments

The UV spectrums were recorded at room temperature on Jasco spectrophotometer equipped with 1.0 cm quartz cells. All fluorescence spectra were recorded on Jasco-55 Spectrofluorimeter equipped with 1.0 cm quartz cells and a thermostat water bath (Julabo, USA).

2.3. Spectroscopic measurements

The absorption spectroscopy of EA was performed at room temperature in phosphate buffer saline. To minimize the contribution of the tyrosine residues fluorescence measurements were carried out at 295 nm excitation wavelength. The spectrum data points were collected from 300 to 425 nm. The widths of both the excitation and the emission slit were set at 2.5 and 6 nm, respectively. Fluorescence measurement was carried out at different temperatures (298, 302, 306 and 310 K). The concentration of HSA was fixed at 5 μM and EA concentration was varied from 0 to 30 μM. Appropriate buffer has been taken as blank and subtracted from the experimental spectrum to correct the background of fluorescence.

2.4. Molecular docking study of EA with HSA

The crystal structure of HSA (Protein Data Bank (PDB) entry 1AO6 [23]) was downloaded from the PDB [24]. Sybyl 6.92 was used to generate the 3D structure of EA and the energy minimized conformation was obtained with the help of the TRIPOS force field using MMFF94 charges with a gradient of 0.005 kcal/mol. The other parameters dielectric constant, iteration number, maximum displacement, minimum energy change, simplex threshold and simplex iteration were set to 1.0, 1000, 0.01, 0.005, 1000 and 20, respectively. FlexX single molecule docking software was used for the docking of EA to HSA. The ranking of the generated solutions is performed using a scoring function as mentioned by Rarey et al. [25], which estimates the free binding energy ΔG of the protein–ligand complex. PyMol [26] was used for visualization and measurement of distances between the ligand and the receptor.

The accessible surface area of HSA and the HSA–EA docked complex were calculated using NACCESS [27]. In this case if a residue lost more than 20 $Å^2$ accessible surface area when going from the non-complexed to the complexed state it was considered as being involved in the interaction.

3. Results and discussions

3.1. Fluorescence characteristics of EA and HSA

Any process, which decreases the fluorescence intensity of a sample, is referred as fluorescence quenching [28]. The basic principles like excited state reactions, molecular rearrangements, energy transfer, ground state complex formation, and collisional quenching involves in molecular interaction, which can result in quenching. Quenching can occur by different mechanisms like dynamic quenching and static quenching. The

mechanism can be distinguished from the differing dependence on temperature and viscosity on the Stern–Volmer constant (K_{SV}) values. Dynamic quenching depends upon diffusion. Since higher temperatures results larger diffusion coefficients, the bimolecular quenching constants are expected to increase with increasing temperature. In contrast, increased temperature is likely to result in decreased stability of complexes, and thus lower values of the static quenching constants [29].

In order to discuss the results within the linear concentration range, we selected carrying out the experiment within the linear part of Stern–Volmer dependence and quenching data were analyzed in terms of Stern–Volmer constant (K_{SV}) which was calculated from the ratio of the unquenched and the quenched fluorescence intensities, F_0/F, using the relationship in the following equation:

$$\frac{F_0}{F} - 1 = K_{SV}[Q] \quad (1)$$

Here Q is the molar concentration of the quencher, F_0 the fluorescence intensity at 0 concentration ligand, F the fluorescence intensity at varied ligand concentration, and $[Q]$ is the quencher concentration.

Concentration of EA varied from (0 to 30) $\times 10^{-6}$ mol L^{-1} fixing the concentrations of HSA at 5.0×10^{-6} mol L^{-1}. As can be seen from Fig. 2, addition of increasing concentrations of EA caused a progressive reduction of the fluorescence intensity, accompanied by a decrease of wavelength emission maximum (λ_{max}) in the HSA spectrum. Thus, the fluorescence was strongly quenched, whereas λ_{max} was reduced from 338 to 329 nm by addition of 30×10^{-6} mol L^{-1} EA. But, this quenching is quantitatively lower then reported interaction of HSA with tannic acid derivatives like tannic acid and gallic acid [22], which may be described because of BSA has greater affinity towards gallotannins rather ellagitannins as reported earlier [30]. This suggests an increased hydrophobicity of the region surrounding the tryptophan site [31–33] in the domain IIA. Emission spectrum of native EA indicates a negligible effect on the intrinsic fluorescence of EA, at 295 nm λ_{ext} (Fig. 2). In case of BSA the increase in hydrophobic region is observed towards the surface area in presence of EA has been reported [22].

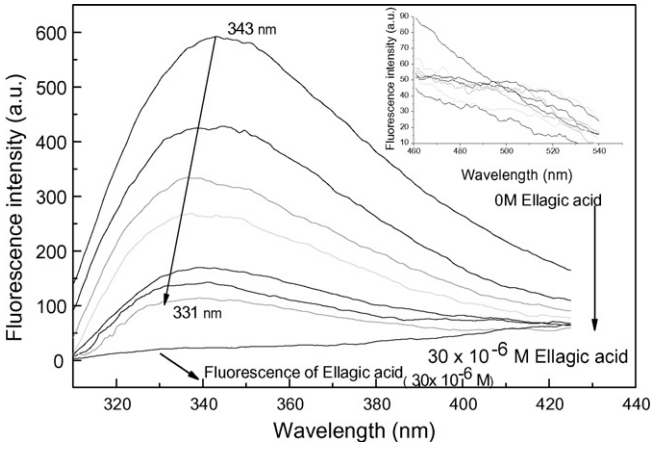

Fig. 2. Fluorescence spectra of the HAS–EA system. The concentration of HSA was 5×10^{-6} M and EA concentration was increased from (0 to 30) $\times 10^{-6}$ M. $T = 302$ K; pH = 7.4 ± 0.1; $\lambda_{ex} = 295$ nm. For the clarity of the spectra at the red-end, it is shown in the insert.

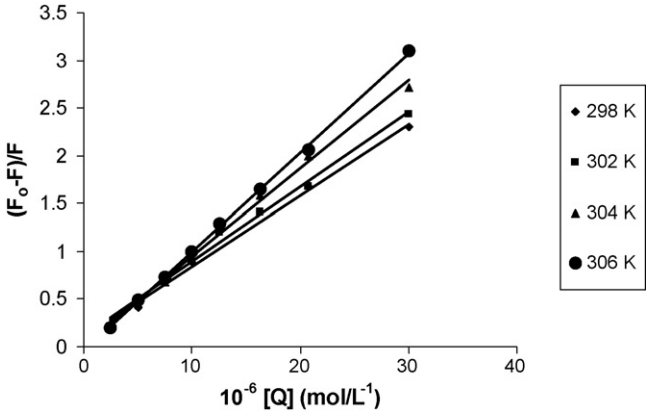

Fig. 3. Stern–Volmer plot of HAS–EA system, at different temperatures concentration of HSA was 5×10^{-6} M, pH 7.4; $\lambda_{ex} = 295$ nm. Temperature is shown as legend in Kelvin unit.

Analysis of Stern–Volmer plots (Fig. 3, Table 1) in this regime yields equilibrium expressions for static quenching (K_a), which are analogous to associative binding constants for the quencher–acceptor system [34]. The binding parameters like association constants K and binding stochiometry n for the HAS–EA complex at 298, 302, 306 and 310 K from fluorescence quenching data were calculated from Scatchard plot (Fig. 4 [35]). The method is based on the general equation:

$$\frac{r}{D_f} = nK - rK \quad (2)$$

where r is the moles of EA bound per mole of protein, D_f the molar concentration of free EA, n the binding stochiometry per class of binding sites, and K is the equilibrium binding constant. The stochiometric studies of tannin protein co-precipitation has been studied and predicted that with the increase in the number of galloyl groups bound increases the BSA precipitatory activities. A two stage mechanism of initial complexation of galloylglucose with BSA and subsequent precipitation has been established [36]. But in the present study, the precipitation does not occur because of the low concentration of macromolecule and ligand.

Fig. 4 displays the Scatchard plots of the HAS–EA system at different temperatures; the corresponding Stern–Volmer quenching constants are calculated and shown in Table 1.

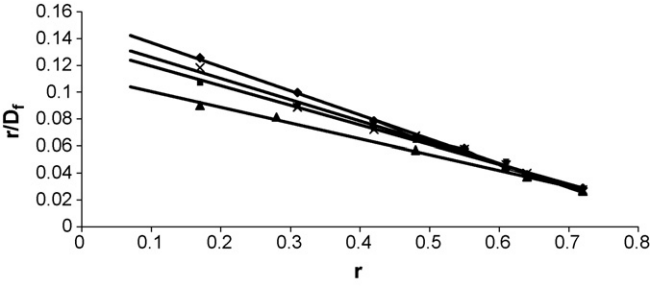

Fig. 4. Scatchard plot for the HAS–EA system. The concentration of HSA was 5 10^{-6} M, T (K) = 298; ♦, 302; ×, 306; ■, 310; ▲; pH = 7.4 ± 0.1; $\lambda_{ex} = 295$ nm.

Table 1
Thermodynamic parameters for EA–HSA system

T (K)	K_{SV}[a] (mM^{-1})	K_a[a] (mM^{-1})	K[a] (mM^{-1})	n	ΔG[a] (kJ mol^{-1})	ΔH (kJ mol^{-1})	ΔS (J mol^{-1} K^{-1})
298	102	79	179	0.862	−6.9		
302	92	76	158	0.895	−6.8	−17.32	34.91
306	81	66	146	0.917	−6.6		
310	79	64	117	0.955	−6.5		

[a] Experimental error ± 5%.

The results show the Stern–Volmer quenching constant K_{SV} is inversely correlated with temperature, which indicates that the probable quenching mechanism of fluorescence of HSA by EA is not initiated by dynamic collision but from complex formation. Therefore, the quenching data were analyzed according to the modified Stern–Volmer plot at four different temperatures (Fig. 5). The modified Stern–Volmer equation [37] is

$$\frac{F_0}{\Delta F} = \frac{1}{f_a K_a} \times \frac{1}{[Q]} + \frac{1}{f_a} \quad (3)$$

In the present case, ΔF is the difference in fluorescence in the absence (F_0) and presence of the quencher F, at concentration $[Q]$, f_a the fraction of the initial fluorescence, which is accessible to the quencher, and K_a is the effective quenching constant.

The dependence of $F_0/\Delta F$ on the reciprocal value of the quencher concentration $[Q]^{-1}$ is linear with slope equal to the value of $(f_a K_a)^{-1}$ (Fig. 5). The value ${f_a}^{-1}$ is fixed on the ordinate. The constant K_a is a quotient of an ordinate ${f_a}^{-1}$ and slope $(f_a K_a)^{-1}$. The corresponding results at different temperatures are shown in Table 1. The decreasing trend of K_a with increasing temperature was in accordance with K_{SV}'s dependence on temperature as mentioned above. It shows that the binding constant between EA and HSA is remarkable and effect of temperature is negligible. A binding constant ($K_{SV} = 75 \pm 16\ mM^{-1}$) of EA with BSA is earlier reported [22]. Thus, it may be concluded that EA can be stored and carried by human serum albumin in the body at physiological conditions.

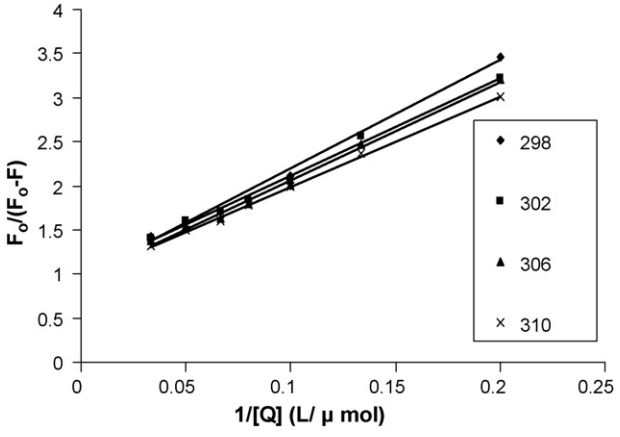

Fig. 5. Modified Stern–Volmer plots of the HAS–EA system: the concentration of HSA: 5×10^{-6} M; pH 7.4 ± 0.1; λ_{ex} = 295 nm, temperature (K) as mentioned in the legend.

3.2. Binding mode and nature of binding site between EA and HSA

The interactions forces between drugs and bimolecule may include electrostatic interactions, multiple hydrogen bonds, van der Waal's interactions, hydrophobic and steric contacts within the antibody-binding site, etc [38]. The binding capacity of drug depends in the strength of interaction (ellagic acid with BSA is 297.3 g/mL [39]). In order to elucidate the interaction of EA with HSA, the thermodynamic parameters were calculated from the van't Hoff plots.

Considering there is not very significant change of enthalpy (ΔH) value over the temperature range studied, the entropy change (ΔS) can be determined from the van't Hoff equation:

$$\ln K = \frac{-\Delta H}{RT} + \frac{\Delta S}{R} \quad (4)$$

where associative binding constants (K) are analogous to the effective quenching constants K_a at the corresponding temperature and R is the gas constant. The temperatures used were 298, 302, 306 and 310 K. The plot of $\ln k$ against $1/T$ is a straight line, the equation of which provides the enthalpy (ΔH) and entropy (ΔS).

The free energy change (ΔG) of binding is estimated from the following relationship:

$$\Delta G = \Delta H - T\Delta S \quad (5)$$

Fig. 6, by fitting the data of Table 1, it shows that assumption of near constant ΔH is justified. Table 1 shows the values of ΔH and ΔS obtained for the binding site from the slopes and ordinates at the origin of the fitted lines. The binding process is

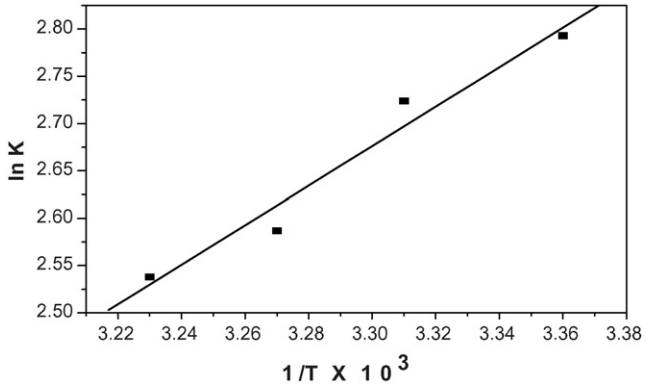

Fig. 6. Temperature dependence of binding constant (van't Hoff plot) at pH 7.4 ± 0.1; HSA concentration: 5.0×10^{-6} M.

spontaneous is evidenced by the negative values of free energy (ΔG) (Table 1).

Van der Waal's interactions and hydrogen bonds play major role in the protein ligand interaction [40,41]. In the present study, the negative values of enthalpy (ΔH) of the interaction of EA and HSA indicate that the binding is mainly enthalpy-driven and the entropy (ΔS) value is unfavorable for it. Hydrogen bonds are specific and directed, which may be best identified through their negative enthalpy of complex formation. HSA is characterized by only one tryptophan residue (Trp214), which is in a well characterized binding cavity (sub-domain IIA) for small charged aromatic molecules [6–10] and [42,43]. The crystallographic analysis of serum albumin also revealed that the major ligand binding sites are identified within this region [43]; it is also known that the binding activity of the sub-domain IIA affects conformational changes [44], which agree with the conformation character mentioned above. Thus, combining this analysis with the structure of EA, we can infer that the binding site for EA on HSA is located in sub-domain IIA (Trp214).

3.3. Molecular docking study of EA with HSA

The experimental observations were followed up with docking studies where EA was docked to HSA to determine the preferred binding site on the protein. The docking pose shown in Fig. 6 shows that EA is located within the binding pocket of sub-domains IIA and IIIA. Trp214 is part of helix 12, which spans residues 208–223. We find that in the best-docked conformation obtained, the indole–NH of Trp214 is within hydrogen bonding distance of the hydroxyl group of EA (3.03 and 4.23 Å, Fig. 7). The C=O moiety of the side chain of Asp 451 of helix 24 comprising residues 444–467 is also within hydrogen bonding distance (2.92 Å) of the hydroxyl group of EA. This is indicative of an ionic contribution to the interaction between HSA and EA as observed in the thermodynamic studies. The $-NH_2$ of Arg 218 form hydrogen bonding with the C=O group of EA within a hydrogen bonding distance 3.02 and 2.75 Å bonding distance from the C atom of the main ring of EA. The $-NH_2$ side group of Arg-222 residue maintains a hydrogen bonding distance of 2.88 Å with the C=O group of EA at the most favorable structure.

To further identify the other residues taking part in the interaction, we calculated the accessible surface area for free HSA and the HSA–EA complex. Residues where the absolute accessible surface areas have decreased by more than 20 $Å^2$ are Lys 195, Trp214, Arg 218, Glu 292, and Asp 451. We find that most of the residues involved in the interaction belong to sub-domains IIA and IIIA as expected from our experimental results. The inside pocket of sub-domain IIA which comprises site I is predominantly hydrophobic in nature with the entrance surrounded by positively charged residues. It has been observed that among these residues Lys 195, Asp 451 and Arg 218 lose the maximum surface area on binding (51.52, 29.26 and 28.33 $Å^2$, respectively). This result provides a good structural basis to explain the very efficient fluorescence quenching of HSA emission in the presence of EA.

3.4. Energy transfer between EA and HSA

In this work, the efficiency of energy transfer was studied according to the Förster resonance energy transfer theory (FRET [45]). The fluorescence quenching of HSA after binding with EA indicated the transfer of energy between EA and HSA has occurred. The efficient ligand–protein interaction gives rise to energy data, from which the distance between two interacting molecules can easily evaluated. The efficiency of energy transfer E, is described by the following equation:

$$E = 1 - \frac{F}{F_0} = \frac{R_0^6}{R_0^6 + r^6} \tag{6}$$

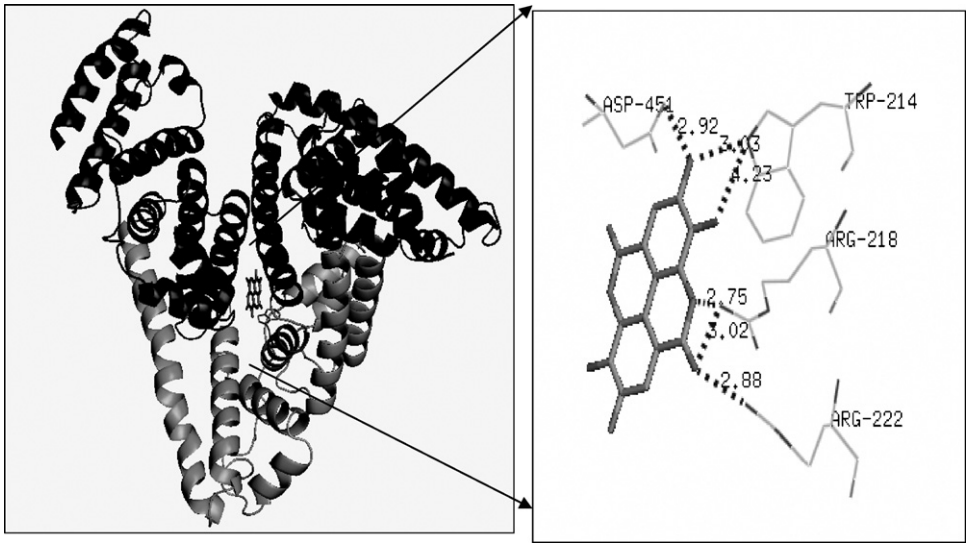

Fig. 7. Schematic representation of the docked pose of EA and HSA (PDB entry 1AO6). The residues of HSA are represented using lines and the EA structure is represented using sticks. The hydrogen bonds between EA and HSA are represented using dashed line. The picture was drawn in PyMol. TRP: Tryptophan, ARG: Arginine, Asp: Aspartate. The number shows the amino acid residue number and the distance is shown in Å unit.

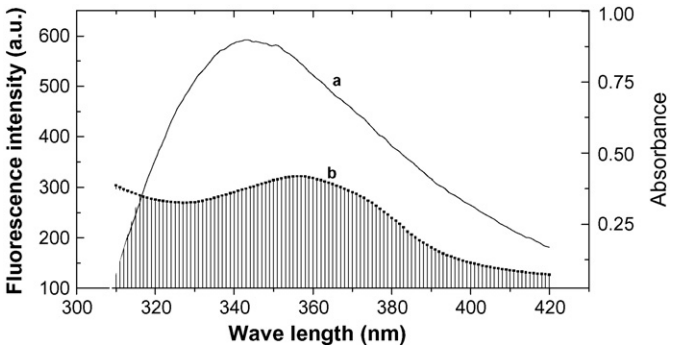

Fig. 8. The overlap of fluorescence emission spectra (a) and the absorption spectra (b) when the molar ratio of EA and HSA ratio is 1:1 and [HSA] = [EA] = 5.0×10^{-6} M, pH = 7.4 ± 0.1.

where F and F_0 are the fluorescence intensities of HSA in the presence and absence of EA, r the distance between acceptor and donor, and R_0 is the critical distance when the transfer efficiency is 50%:

$$R_0^6 = 8.8 \times 10^{-25}\, K^2\, N^{-4}\, \Phi J \tag{7}$$

where K^2 is the spatial orientation factor of the dipole, N the refractive index of the medium, Φ the fluorescence quantum yield of the donor, J is the overlap integral of the fluorescence emission spectrum of the donor and the absorption spectrum of the acceptor. J is given by

$$J = \frac{\sum F(\lambda)\varepsilon(\lambda)\lambda^4 \Delta\lambda}{\sum F(\lambda)\Delta\lambda} \tag{8}$$

where $F(\lambda)$ is the fluorescence intensity of the fluorescent donor at wavelength λ, and $\varepsilon(\lambda)$ is the molar absorption coefficient of the acceptor at wavelength λ. From the above relationships, J and E can be easily obtained; therefore, R_0 and r can be further calculated. Fig. 8 showed the overlap of the fluorescence spectrum of HSA and the absorption spectrum of EA when the molar ratio of EA to HSA is 1:1. J was obtained to be 9.692×10^{-15} cm^3 M^{-1} by integrating the overlap of the UV absorption spectrum of EA and the fluorescence emission spectrum of HSA (Fig. 7), and E was calculated to be 0.81.

It was reported earlier that $K_2 = 2/3$, $\Phi = 0.118$, $N = 1.336$ for HSA [46]. Based on these data, we found $R_0 = 2.5$ nm and $r = 1.96$ nm. So the distance between EA and tryptophan residue in HSA is 1.96 nm, which is far lower than 7 nm [47]. This obeys the conditions of Förster energy transfer theory.

4. Conclusions

The interaction between EA and HSA was studied by fluorescence and UV–vis absorption spectroscopy under similar physiological conditions revealed, the quenching of HSA was by static quenching mechanism. The mode of binding reaction was spontaneous, and the probable binding domain of EA was at the hydrophobic pocket located in sub-domain IIA. The distance between Trp214 and bound EA was calculated using FRET analysis for the first time. Weak interactions like van der Waal's interactions and hydrogen bonding played major role in this reaction. The mode of binding of EA with HSA may be further investigated by a crystal structure of the complex. The effect of mutations of the crucial residues that interact with HSA can be explored. This present study on the interaction of EA with HSA will open up new vistas in drug designing.

Acknowledgements

Financial support of Council of Scientific and Industrial Research (CSIR), New Delhi, India, to Ranjan Kumar Nanda (SRF) is gratefully acknowledged. Prof. Swagata Dasgupta, IIT-Kharagpur, Chemistry Department, is acknowledged for carrying out the molecular docking study.

References

[1] A.O. Pedersen, K.-L.D. Mensberg, U. Kragh-Hansen, Effects of ionic strength and pH on the binding of medium-chain fatty acids to human serum albumin, Eur. J. Biochem. 233 (1995) 395–405.
[2] T. Peters, All about Albumin: Biochemistry, Genetics, and Medical Applications, Academic Press, New York, 1996.
[3] D.C. Carter, J.X. Ho, Structure of serum albumin, Adv. Protein Chem. 45 (1994) 153–203.
[4] G. Sudlow, D.J. Birkett, D.N. Wade, The characterization of two specific drug binding sites on human serum albumin, Mol. Pharmacol. 11 (1975) 824–832.
[5] S. Curry, H. Mandelkow, P. Brick, N. Franks, Crystal structure of human serum albumin complexed with fatty acid reveals an asymmetric distribution of binding sites, Nat. Struct. Mol. Biol. 5 (9) (1998) 827–835.
[6] A.A. Bhattacharya, T. Grüne, S. Curry, Crystallographic analysis reveals common modes of binding of medium and long-chain fatty acids to human serum albumin, J. Mol. Biol. 303 (5) (2000) 721–732.
[7] X.M. He, D.C. Carter, Atomic structure and chemistry of human serum albumin, Nature 358 (6383) (1992) 209–215.
[8] T. Peters Jr., Serum albumin, Adv. Protein Chem. 37 (1985) 161–245.
[9] S. Curry, P. Brick, N.P. Franks, Fatty acid binding to human serum albumin: new insights from crystallographic studies, Biochem. Biophys. Acta 1441 (2–3) (1999) 131–140.
[10] I. Petitpas, T. Grüne, A.A. Bhattacharya, S. Curry, Crystal structures of human serum albumin complexed with monounsaturated and polyunsaturated fatty acids, J. Mol. Biol. 314 (5) (2001) 955–960.
[11] D.C. Carter, B. Chang, J.X. Ho, K. Keeling, Z. Krishnasami, Preliminary crystallographic studies of four crystal forms of serum albumin, Eur. J. Biochem. 226 (3) (1994) 1049–1052.
[12] J.L. Perry, Y.V. Il'ichev, V.R. Kempf, J. McClendon, G. Park, R.A. Manderville, F. Ruker, M. Dockal, J.D. Simon, Binding of ochratoxin A derivatives to human serum albumin, J. Phys. Chem. B 107 (27) (2003) 6644–6647.
[13] Q. Bian, J. Liu, J. Tian, Z. Hu, Binding of genistein to human serum albumin demonstrated using tryptophan fluorescence quenching, Int. J. Biol. Macromol. 34 (2004) 275–279.
[14] R.E. Olson, Evolution of ideas about the nutritional value of dietary fat: introduction, J. Nutr. 128 (Suppl. 2) (1998) 421S–422S.
[15] M. Falsaperla, G. Morgia, A. Tartarone, R. Ardito, G. Romano, Support ellagic acid therapy in patients with hormone refractory prostate cancer (HRPC) on standard chemotherapy using vinorelbine and estramustine phosphate, Eur. Urol. 47 (4) (2005) 449–454.
[16] C. Han, H. Ding, B. Casto, G.D. Stoner, S.M. D'Ambrosio, Inhibition of the growth of premalignant and malignant human oral cell lines by extracts and components of black raspberries, Nutr. Cancer 51 (2) (2005) 207–217.
[17] E.H. Kang, T.Y. Kown, G.T. Oh, W.F. Park, S.-I. Park, S.K. Park, Y.I. Lee, The flavonoid ellagic acid from a medicinal herb inhibits host immune tolerance induced by the hepatitis B virus-e antigen, Antivir. Res. 72 (2) (2006) 100–106.

[18] K.L. Khanduja, P.K. Avti, S. Kumar, N. Mittal, K.K. Sohi, C.M. Pathak, Anti-apoptotic activity of caffeic acid, ellagic acid and ferulic acid in normal human peripheral blood mononuclear cells: a Bcl-2 independent mechanism, Biochem. Biophys. Acta 1760 (2) (2006) 283–289.
[19] G. Cozza, P. Bonvini, E. Zorzi, G. Poletto, M.A. Pagano, S. Sarno, A. Donella-Deana, G. Zagotto, A. Rosolen, L.A. Pinna, F. Meggio, S. Moro, Identification of ellagic acid as potent inhibitor of protein kinase CK2: a successful example of a virtual screening application, J. Med. Chem. 49 (8) (2006) 2363–2366.
[20] B.A. Narayanan, G.G. RE, IGF-II down regulation associated cell cycle arrest in colon cancer cells exposed to phenolic antioxidant ellagic acid, Anticancer Res. 21 (1A) (2001) 359–364.
[21] Z. Papoutsi, E. Kassi, A. Tsiapara, N. Fokialakis, G.P. Chrousos, P. Moutsatsou, Evaluation of estrogenic/antiestrogenic activity of ellagic acid via the estrogen receptor subtypes ERα and ERβ, J. Agric. Food Chem. 53 (20) (2005) 7715–7720.
[22] M. Labieniec, T. Gabryelak, Interactions of tannic acid and its derivatives (ellagic and gallic acid) with calf thymus DNA and bovine serum albumin using spectroscopic method, J. Photochem. Photobiol. B 82 (1) (2006) 72–78.
[23] S. Sugio, A. Kashima, S. Mochizuki, M. Noda, K. Kobayashi, Crystal structure of human serum albumin at 25 Å resolution, Protein Eng. 12 (6) (1999) 439–446.
[24] M. Berman, J. Westbrook, Z. Feng, G. Gilliland, T.N. Bhat, H. Weissig, I.N. Shindyalov, P.E. Bourne, The protein data bank, Nucl. Acids Res. 28 (1) (2000) 235–242.
[25] M. Rarey, B. Kramer, T. Lengauer, G. Klebe, A fast flexible docking method using an incremental construction algorithm, J. Mol. Biol. 261 (1996) 470–489.
[26] W.L. DeLano, The PyMOL Molecular Graphics System, DeLano Scientific, San Carlos, CA, USA, 2004.
[27] S.J. Hubbard, J.M. Thornton, 'NACCESS' Computer Program, Department of Biochemistry and Molecular Biology, University College London, 1993.
[28] J.R. Lakowicz, Principles of Fluorescence Spectroscopy, 2nd ed., Plenum Press, New York, 1999, pp. 237.
[29] Y.J. Hu, Y. Liu, R.-M. Zhao, S.-S. Qu, Interaction of colchicine with human serum albumin investigated by spectroscopic methods, Int. J. Biol. Macromol. 37 (2005) 122–126.
[30] K.S. Feldman, A. Sambandam, S.T. Lemon, R.B. Nicewonger, G.S. Long, D.F. Battaglia, S.M. Ensel, M.A. Laci, Binding affinities of gallotannin analogs with bovine serum albumin: ramifications for polyphenol-protein molecular recognition, Phytochemistry 51 (1999) 867–872.
[31] M. Dockal, D.C. Carter, F. Rüker, Conformational transitions of the three recombinant domains of human serum albumin depending on pH, J. Biol. Chem. 275 (2000) 3042–3050.
[32] U. Kragh-Hansen, F. Hellec, B. de Foresta, M. le Maire, J.V. Møller, Detergents as probes of hydrophobic binding cavities in serum albumin and other water-soluble proteins, Biophys. J. 80 (2001) 2898–2911.
[33] Y.V. Il'ichev, J.L. Perry, J.D. Simon, Interaction of ochratoxin A with human serum albumin preferential binding of the dianion and pH effects, J. Phys. Chem. B 106 (2) (2002) 452–459.
[34] L. Pu, Fluorescence of organic molecules in chiral recognition, Chem. Rev. 104 (3) (2004) 1687–1716.
[35] G. Scatchard, The attractions of proteins for small molecules and ions, Ann. N.Y. Acad. Sci. 51 (1949) 660–672.
[36] H. Kawamoto, F. Nakatsubo, K. Murakami, Stoichiometric studies of tannin-protein co-precipitation, Phytochemistry 41 (5) (1996) 1427–1431.
[37] S.S. Lehrer, Solute perturbation of protein fluorescence. Quenching of the tryptophyl fluorescence of model compounds and of lysozyme by iodide ion, Biochemistry 10 (17) (1971) 3254–3263.
[38] D. Leckband, Measuring the forces that control protein interactions, Annu. Rev. Biophys. Bimol. Struct. 29 (2000) 1–26.
[39] R.K. Dawra, H.P.S. Makkar, B. Singh, Protein-binding capacity of microquantities of tannins, Anal. Biochem. 170 (1988) 50–53.
[40] P.D. Ross, S. Subramanian, Thermodynamics of protein association reactions: forces contributing to stability, Biochemistry 20 (11) (1981) 3096–3102.
[41] S.N. Timaseff, Proteins of Biological Fluids, Pergamon Press, Oxford, 1972, pp. 511–519.
[42] U. Kragh-Hansen, Molecular aspects of ligand binding to serum albumin, Pharmacol. Rev. 33 (1981) 17–53.
[43] D.C. Carter, X.M. He, Structure of human serum albumin, Science 249 (1990) 302–303.
[44] P. Miskovsky, D. Jancura, S. Sanchez-Cortes, E. Kocisova, L. Chinsky, Antiretrovirally active drug hypericin binds the IIA subdomain of human serum albumin: resonance raman and surface-enhanced raman spectroscopy study, J. Am. Chem. Soc. 120 (25) (1998) 6374–6379.
[45] T. Orster, O. Sinaoglu (Eds.), Modern Quantum Chemistry, vol. 3, Academic Press, New York, 1966.
[46] F.L. Cui, J. Fan, D.L. Ma, M.C. Liu, X.G. Chen, Z.D. Hu, A study of the interaction between a new reagent and serum albumin by fluorescence spectroscopy, Anal. Lett. 36 (10) (2003) 2151–2166.
[47] F.L. Cui, J. Fan, J. Ping Li, Z. Hu, Interactions between 1-benzoyl-4-*p*-chlorophenyl thiosemicarbazide and serum albumin: investigation by fluorescence spectroscopy, Bioorg. Med. Chem. 12 (2004) 151–157.